Supplementary Information (SI) for Nanoscale Horizons.
This journal is © The Royal Society of Chemistry 2024

Intravital Microscopic Thermometry of Rat Mammary Epithelium by Fluorescent Nanodiamond

Takahiro Hamoya, Kiichi Kaminaga, Ryuji Igarashi, Yukiko Nishimura, Hiromi Yanagihara, Takamitsu Morioka, Chihiro Suzuki, Hiroshi Abe, Takeshi Ohshima, Tatsuhiko Imaoka

EXPERIMENTAL

To determine the concentration of NVCs in FNDs, we conducted measurements using electron spin resonance (ESR) spectroscopy. In NVCs with a spin quantum number of $S = 1$, a forbidden transition with a change in the spin magnetic quantum number $\Delta m_s = 2$ occurs, leading to the detection of the half-field transition signal at approximately half the magnetic field strength of the regular ESR field. This half-field transition is observed in the region where the effective g-factor $g_{eff} \approx 4$. In FND powder, the spin orientation is randomly distributed, making it difficult to detect the usual transition ($\Delta m_s = 1$). However, the half-field transition is less affected by orientation and thus provides a stable signal intensity. Therefore, we evaluated the concentration of NVCs in FNDs based on the intensity of the half-field transition. As a result, the concentration of NVCs was estimated to be ~1.7 ppm. Assuming a nanodiamond as a spherical particle with a diameter of 200 nm, the average number of NVCs per particle was calculated to be $\sim 1.3 \times 10^3$.

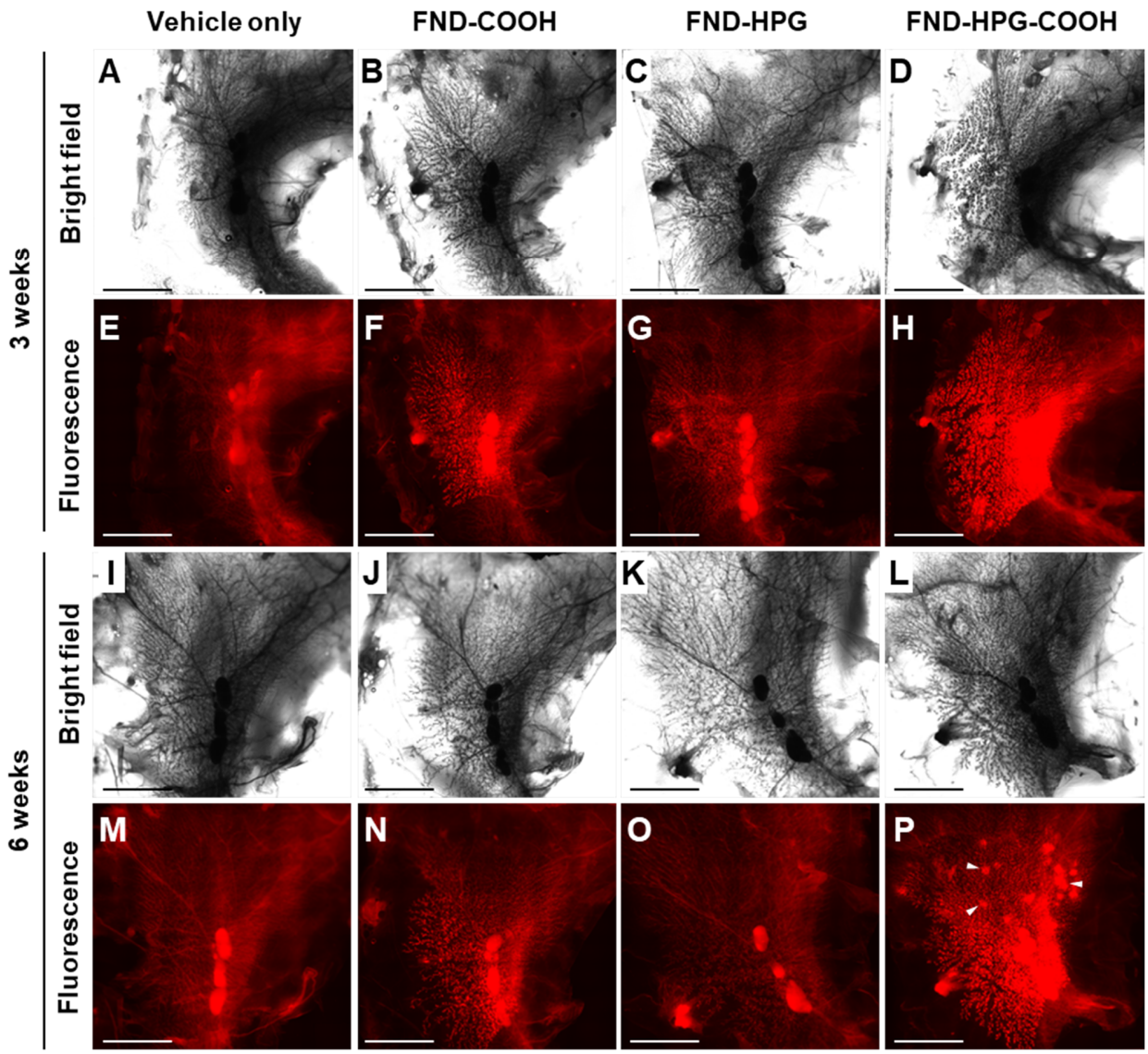

Figure S1. Presence of intraductally injected FNDs in the mammary gland of rats after 3 and 6 weeks. Bright-field (A–D and I–L) and fluorescence (E–H and M–P) images of the whole-mount mammary gland specimens at 3 and 6 weeks post-injection. White arrowheads show a mass of FNDs. Scale bar, 1 mm.

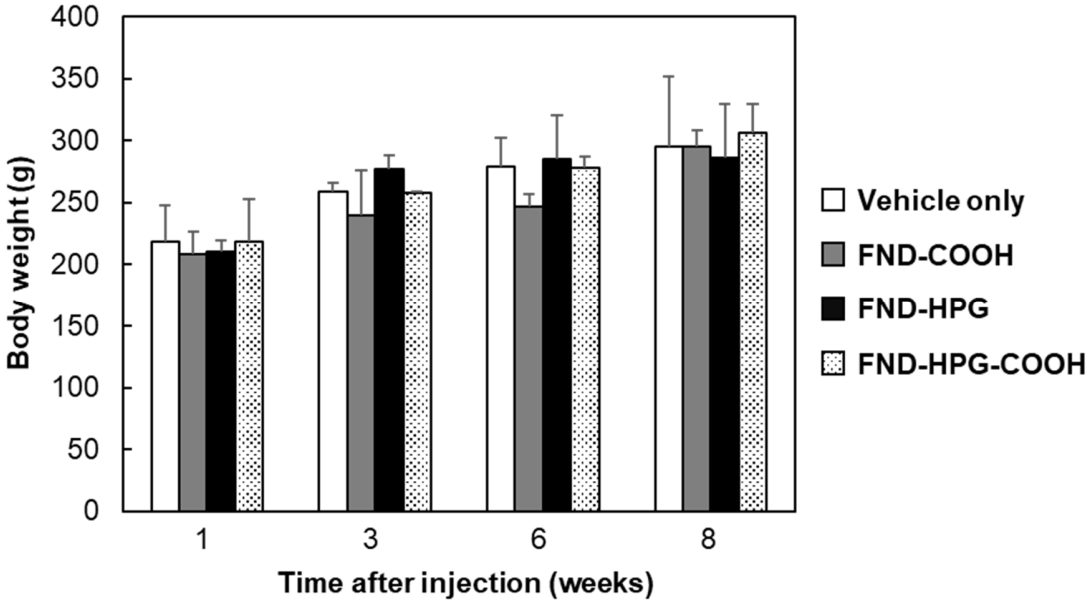

Figure S2. Effect of intraductal FND injection on the body weight. Body weight was measured at 1, 3, 6, and 8 weeks post-injection of vehicle only (A and E) or FND-X (X = COOH, HPG, or HPG-COOH). Data represent the mean and SD (n = 3 rats).

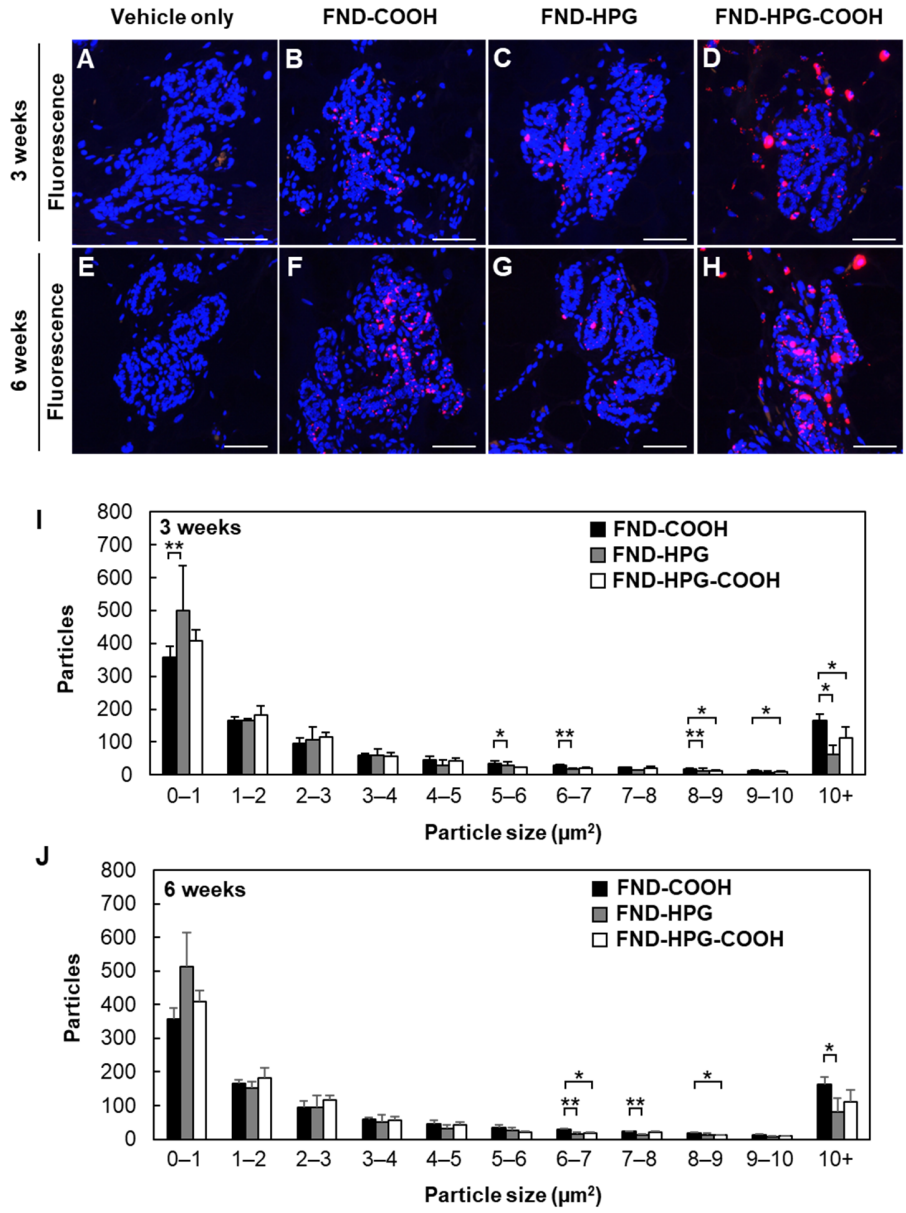

Figure S3. Localization of intraductally injected FNDs in the mammary epithelium of rats at 3 and 6 weeks. A–H. Fluorescence images of DAPI-stained mammary epithelial cells at 3 and 6 weeks post-injection injection of vehicle only (A and E) or FND-X (X = COOH in B and F, HPG in C and G, and HPG-COOH in D and H). Scale bar, 50 μm. **I and J.** The size of FND aggregates (n = 1,000) in the mammary epithelium at 3 (I) and 6 weeks (J) post-injection. Ranges do not include the lower boundary. Data represent the mean and SD (n = 3 rats). * $P < 0.05$, ** $P < 0.01$ (Student's t test).

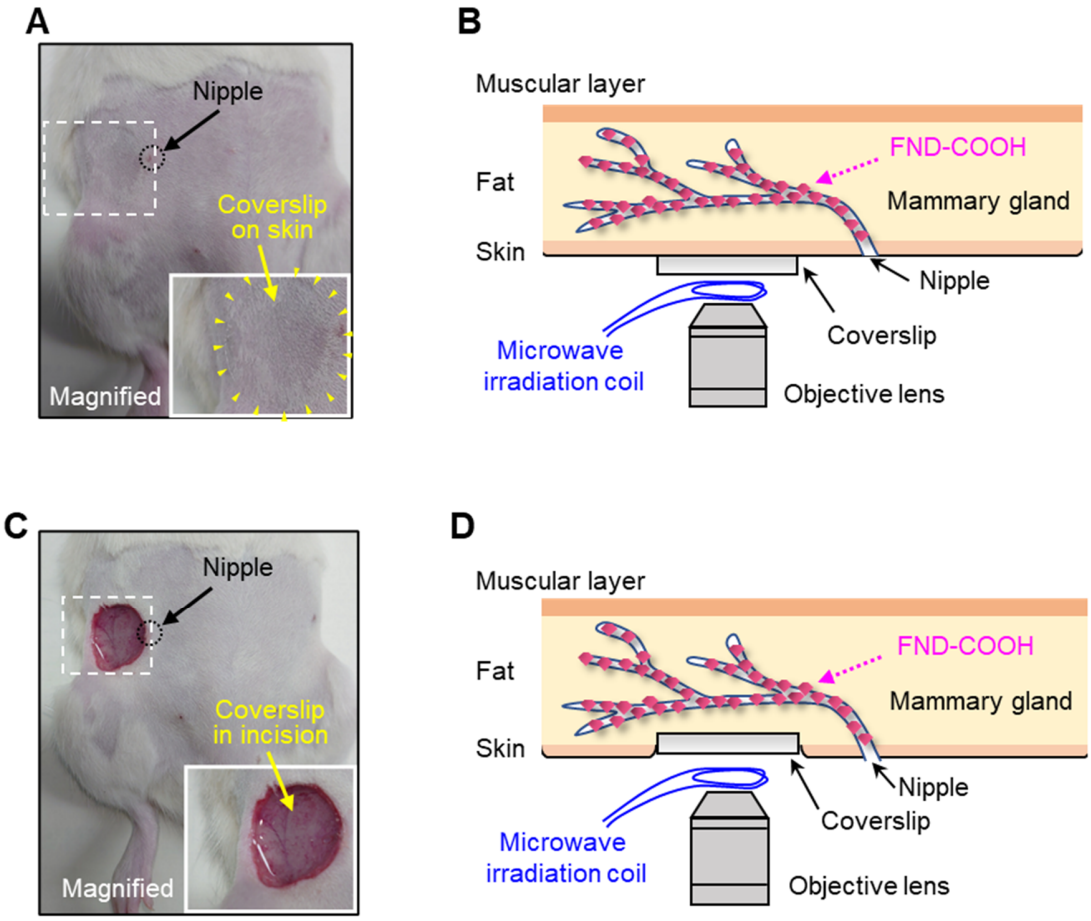

Figure S4. Setup for intravital observation of FNDs in the rat mammary gland. A and B. Observation through the skin. **C and D.** Observation through a skin incision. Photographs (A and C) and schematics (B and D) are shown. Insets in panels A and C show magnified views of the area bounded by dashed rectangles. Yellow arrowheads show the outline of a round coverslip.

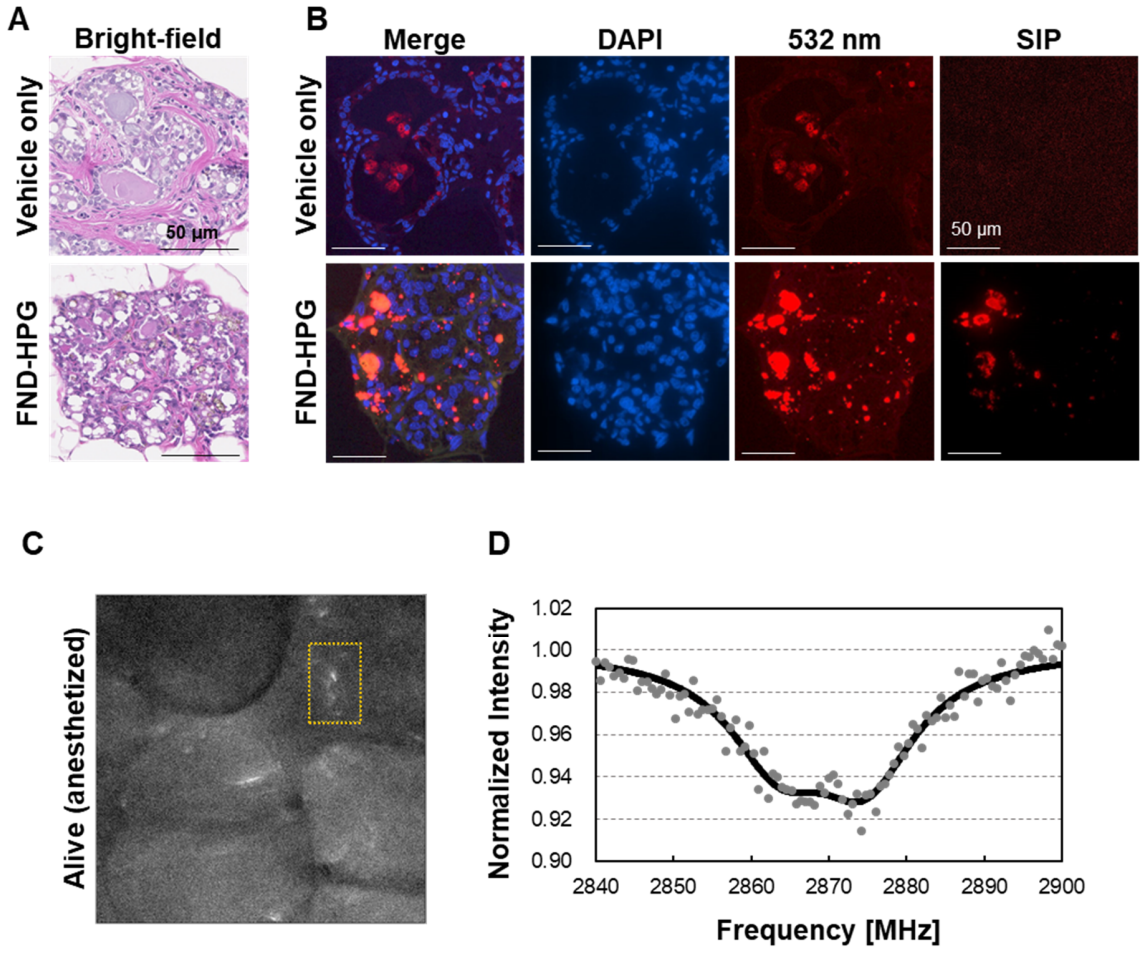

Figure S5. Rat mammary gland at 1 year post-injection of FNDs. FND-HPG (200 in diameter) were intraductally injected into the mammary gland of 7-week-old rats, and the presence of FNDs was assessed 1 year later. **A.** HE staining of mammary gland sections indicates no obvious toxicity. **B.** Fluorescence image of mammary gland tissue sections. DAPI, cell nuclei. 532 nm, fluorescence at 532 nm. Signals in the upper panel are due to autofluorescence. SIP, fluorescence from FNDs identified as microwave-sensitive components. **C.** Fluorescence image (with 20× objective lens, excitation 532 nm) of the mammary gland *in vivo*. Fluorescence is diffused by mammary fat cells that had grown fully by this age. **D.** ODMR spectrum of the yellow rectangular field shown in panel C. Scale bars in A and B, 50 μm.